ESTIMATION OF THE TURBULENCE ENERGY DISSIPATION RATE FROM THE PULSED DOPPLER LIDAR DATA

V.A. Banakh and I.N. Smalikho

Institute of Atmospheric Optics,
Siberian Branch of the Russian Academy of Sciences, Tomsk
Received August 1, 1997

Based on the results of numerical modeling we have analyzed the possibility and calculated the errors of estimating turbulence kinetic energy dissipation rate from data of pulsed Doppler lidar. Compared are the accuracies of estimation of wind velocity spatial structure function from Doppler lidar data obtained by the method of correlation function argument and the method of maximum likelihood. It is shown that, when using sufficiently large number of sample data, the relative error in estimation of turbulence energy dissipation rate with a pulsed Doppler lidar must be below 15–20% *at signal-to-noise ratio equal or greater than unity.*

1. INTRODUCTION

Doppler lidars with a pulsed radiation source are now more and more widely used to study atmospheric processes.[1–8] The reason is that these lidars allow reconstructing altitude profiles of parameters measured with high spatial resolution up to significantly higher altitudes than cw lidars. At the same time, the problems of accuracy to which turbulent characteristics are measured with pulse lidars using different processing methods are still open and require further research.

One of the most important characteristics of turbulence is the kinetic energy dissipation rate ε. The methods of measuring ε in the boundary atmospheric layer with continuous lidars are considered in Refs. 9–13, where the problems of influence of spatial averaging over sounded volume on the characteristics of wind velocity measured with the lidar and the problems of taking into account this averaging in lidar measurements of dissipation rate are discussed in great detail. This paper is devoted to study of possibilities to obtain information about turbulent energy dissipation rate from the data of a pulsed Doppler lidar.

2. CORRELATION FUNCTION OF THE COHERENTLY DETECTED SIGNAL

When sounding with a pulsed lidar, the signal component of photocurrent j_s measured at the moment t can be presented as[14,15]

$$j_s(t) = \mathrm{Re}\,\{y(t)\}, \qquad (1)$$

where

$$y(t) = 2\,\frac{e\,\eta_Q}{h\nu}\,\frac{K(R)}{R}\,P_L^{1/2}\sum_{l=1}^{n_s} P_T^{1/2}\,(t - 2z_l/c)\,\alpha_l \times$$

$$\times\, Q(\rho_l)\,\exp\left[2jkz_l + 2\pi j\left(\Delta f - \frac{2}{\lambda}\,V_r(z_l)\right)t\right];$$

$$Q(\rho_l) = R\lambda \int_{-\infty}^{\infty} d^2\rho W(\rho)\,A_L^*(\rho) \int_{-\infty}^{\infty} d^2\rho' A_T(\rho') W(\rho') \times$$

$$\times\, G(\rho_l, R; \rho', 0)\,G(\rho_l, R; \rho, 0),$$

n_s is the number of scatterers in the atmosphere, $R = ct/2$ is the distance to sounded volume, c is the speed of light, e is the electron charge, η_Q is the quantum efficiency of the photodetector's sensitive area, $h\nu$ is the photon energy, $K(R) = \exp\left\{-\int_0^R dz'\alpha_a(z')\right\}$, α_a is the extinction coefficient, $A_L(\rho) = E_L(\rho)/P_L^{1/2}$ and $A_T(\rho) = E_T(\rho, t)/P_T^{1/2}(t)$ are normalized amplitudes, $P_T(t) = \int_{-\infty}^{\infty} d^2\rho |E_T(\rho, t)|^2$ and $P_L = \int_{-\infty}^{\infty} d^2\rho |E_L(\rho)|^2$ are the sounding and reference beam power, respectively, $U_P = \int_{-\infty}^{\infty} dt\, P_T(t)$ is the energy of a sounding pulse, α_l is the scattering amplitude of lth particle being at the point $\{z_l, \rho_l\}$ (z is the propagation axis), $W(\rho)$ is the pupil function of transceiving telescope, G is the Green's function, $k = 2\pi/\lambda$; λ is the sounding radiation wavelength, Δf is intermediate frequency, and $V_r(z)$ is the radial wind velocity component at the distance z from the lidar.

For the average value of the signal component of photocurrent $S = (1/2)\,\overline{y(t)y^*(t)}$ from Eq. (1) we have[14]

$$S = 2\,[e\eta_Q/(h\nu)]^2\,P_S P_L \eta_H, \qquad (2)$$

where $P_S = A_R\,\beta_\pi(R)\,K^2(R)\,cU_P/(2R^2)$ is the power of signal detected in an incoherent detection mode,

0235-6880/97/12 957-09 $02.00

$A_R = \int_{-\infty}^{\infty} d^2\rho W^2(\rho)$ is the aperture area of the transceiving telescope, $\beta_\pi = \overline{\alpha_l^2}\ \rho_c$ is backscattering coefficient, ρ_c is the particle concentration, $\eta_H = A_R^{-1} \int_{-\infty}^{\infty} d^2\rho_l \overline{|Q(\rho_l)|^2}$ is the heterodyning efficiency.

Along with the signal component $y(t)$, the lidar receiving system records also the photocurrent noise component $n(t)$. In the case, when the shot noise due to the random character of reference radiation photons capture by electrons (the process described by the Poison statistics) is the main source of noise, for the average noise power $N = \overline{|n|^2}$ we have[16]

$$N = 2\, e^2 \eta_Q\, P_L B/(h\nu), \tag{3}$$

where B is the receiver bandpass. The expression for signal-to-noise ratio $SNR = S/N$ can be presented as

$$SNR = \eta_Q \eta_H P_S/(h\nu B). \tag{4}$$

The parameter SNR is the average number of photoelectrons detected coherently for the time $\sim B^{-1}$ (Ref. 17).

From the sequence of photocurrent pulses recorded with lidar we can go to the complex signal

$$Z(mT_S) = (1/\sqrt{2})\, y(t + mT_S) + n(mT_S), \tag{5}$$

where $T_S = B^{-1}$ is the time of complex signal recording. The signal $Z(mT_S)$ obeys the relations

$$\overline{Z(mT_S)} = \overline{Z(mT_S)Z(lT_S)} = 0;$$

$$\overline{Z(mT_S)Z^*(lT_S)} = SK_y(mT_S, lT_S) + N\delta_{ml},$$

where K_y is the correlation coefficient of the complex value of signal (this coefficient is obtained by averaging the function $y(t + mT_S)\ y^*(t + lT_S)$ over all random medium parameters except for wind velocity), δ_{ml} is the Kronecker symbol ($\delta_{ml,m=l} = 1$, $\delta_{ml,m\neq l} = 0$).

Separation of Doppler frequency f_D from the measured sequence $Z(mT_S)$ can be done only within the Nyqist range $[0.1/T_S]$. Having come from $Z(mT_S)$ to $Z(mT_S) \exp[-2\pi j \Delta f m T_S]/\sqrt{N}$ and taking $\Delta f = 1/(2T_S)$, with regard to the Doppler relation $V_D(R) = (\lambda/2) f_D$, we obtain that the estimation of the radial wind speed $V_D(R)$ is within the range $[-\lambda/(4T_S), \lambda/(4T_S)]$. After such a transformation, from Eqs. (1)–(5) for the correlation function of the complex signal $B_z(mT_S, lT_S) = \overline{Z(mT_S)\, Z^*(lT_S)}$ we have the following expression:

$$B_z(mT_S, lT_S) = SNR\ 2\ /\ cU_P \times$$

$$\times \int_{-\infty}^{\infty} dz'\, P_T^{1/2}(mT_S - 2z'/c)\, P_T^{1/2}\,(lT_S - 2z'/c) \times$$

$$\times \exp\left[j \frac{4\pi}{\lambda} (l - m)\, T_S V_r (R + z') \right] + \delta_{ml}. \tag{6}$$

In the case of homogeneous wind $V_r = \text{const}$ and Gaussian shape of sounding pulse

$$P_T(t) = (U_P/\sqrt{\pi\sigma})\, e^{-t^2/\sigma^2}, \tag{7}$$

where $\sigma = t_P$ is the pulse duration determined from the equation $P_T(t_P)\ /\ P_T(0) = e^{-1}$, we have[15,17] from Eq. (6)

$$B_z(mT_S, lT_S) = B_z((m - l)T_S) =$$

$$= SNR \exp\{-[(m - l)T_S/(2\sigma)]^2 -$$

$$-j\,(4\pi/\lambda)\,(m - l)T_S V_r\} + \delta_{ml}. \tag{8}$$

3. ESTIMATION OF THE RADIAL WIND VELOCITY

There are several methods for estimation of radial wind velocity $V_D(R)$ from the measured sequence $Z(mT_S)$, where $m = 0,1, \ldots, M-1$. Considered below are two estimation methods: the correlation function argument (CFA) method and the maximum likelihood (ML) method.

3.1. Estimation of the radial wind velocity by the correlation function argument method

When using the CFA method the velocity is estimated as[18]

$$V_D(R) = \lambda \arg[\hat{B}_z(T_S)]/(4\pi T_S), \tag{9}$$

where $\hat{B}_z(T_S) = \frac{1}{M-1} \sum_{i=0}^{M-2} Z(iT_S)\, Z^*((i + 1)T_S)$ is unbiased estimate of the correlation function of signal with time shift T_S. Let us find the value of such an estimate $\overline{B_z(T_S)} = (M-1)^{-1} \sum_{i=0}^{M-2} \overline{Z(iT_S)Z^*((i+1)T_S)}$. The conditions $M \gg 1$ and $t_P \gg T_S$ allow us to come from the sum on i to integration in time and, based on Eq. (6), to obtain the expression:

$$\overline{B_z(T_S)} = \frac{SNR}{U_P} \int_{-\infty}^{\infty} dt\, P_T(t)\, \frac{1}{\tau} \times$$

$$\times \int_{-\tau/2}^{\tau/2} dt'\, \exp\left[j \frac{4\pi}{\lambda} T_S V_r \left(R + \frac{c}{2}(t + t')\right)\right], \tag{10}$$

where $\tau = MT_S$. Let the velocity estimate obtained with the use of Eq. (9) satisfies the inequality $-\lambda/(8T_S) < V_D(R) < \lambda/(8T_S)$, then $V_D(R)$ can be presented as

$$V_D(R)=\frac{\lambda}{4\pi T_S}\arctan\left\{\frac{\int\limits_{-\infty}^{\infty}dtP_T(t)\int\limits_{-\tau/2}^{\tau/2}dt'\sin\left[\frac{4\pi}{\lambda}T_SV_r(R+\frac{c}{2}(t+t'))\right]}{\int\limits_{-\infty}^{\infty}dtP_T(t)\int\limits_{-\tau/2}^{\tau/2}dt'\cos\left[\frac{4\pi}{\lambda}T_SV_r(R+\frac{c}{2}(t+t'))\right]}\right\}+V_e(R), \quad (11)$$

where

$$V_e(R)=\frac{\lambda}{4\pi T_S}\arctan\left\{\frac{\mathrm{Im}[\hat{B}_z(T_S)\,\overline{B_z(T_S)}^{\,*}]}{\mathrm{Re}[\hat{B}_z(T_S)\,\overline{B_z(T_S)}^{\,*}]}\right\} \quad (12)$$

is the error of velocity estimate due to signal fluctuations and noise. To simplify the first term in Eq. (11), let us introduce a small parameter $\mu(t+t')=(4\pi/\lambda)\,T_S[V_r(R+(t+t')\,c/2)-V_a(R)]$, where $V_a(R)$ is the velocity value closest to values V_r within the sounding range, expand numerator and denominator into a series over this parameter, restricting ourselves to the second-power terms

$$\int\limits_{-\infty}^{\infty}dt\,P_T(t)\int\limits_{-\tau/2}^{\tau/2}dt'\sin(\beta+\mu)\approx$$

$$\approx\int\limits_{-\infty}^{\infty}dt\,P_T(t)\int\limits_{-\tau/2}^{\tau/2}dt'\,[\sin\beta+\mu\cos\beta-(1/2)\,\mu^2\sin\beta];$$

$$\int\limits_{-\infty}^{\infty}dt\,P_T(t)\int\limits_{-\tau/2}^{\tau/2}dt'\cos(\beta+\mu)\approx$$

$$\approx\int\limits_{-\infty}^{\infty}dt\,P_T(t)\int\limits_{-\tau/2}^{\tau/2}dt'[\cos\beta-\mu\sin\beta-(1/2)\mu^2\cos\beta],$$

where

$\beta=(4\pi/\lambda)\,T_SV_a(R)$. Having imposed the condition

$$\int\limits_{-\infty}^{\infty}dt\,P_T(t)\int\limits_{-\tau/2}^{\tau/2}dt'\,\mu(t+t')=0, \quad (13)$$

we come to the expression

$$V_D(R)=V_a(R)+V_e(R), \quad (14)$$

then having solved Eq. (13) we have for $V_a(R)$

$$V_a(R)=\frac{1}{U_P}\int\limits_{-\infty}^{\infty}dt\,P_T(t)\,\frac{1}{\tau}\int\limits_{-\tau/2}^{\tau/2}dt'\,V_r\left[R+\frac{c}{2}(t+t')\right]. \quad (15)$$

Equation (14) is valid, if the inequality

$$\sqrt{\sigma_r^2-\sigma_a^2}\ll\lambda/(8T_S) \quad (16)$$

holds true, where $\sigma_r^2=\langle[V_r(R)-\langle V_r(R)\rangle]^2\rangle$ and $\sigma_a^2=\langle[V_a(R)-\langle V_a(R)\rangle]^2\rangle$ are the variances of radial wind velocity at a point and averaged over the volume sounded, respectively. Condition (16) is true practically always.

In the case of a Gaussian pulse (7), it follows from Eq. (15) that:

$$V_a(R)=\int\limits_{-\infty}^{\infty}dz'\,Q_S(z')\,V_r(z'), \quad (17)$$

where

$$Q_S(z')=\frac{1}{\tau c}\left[\mathrm{erf}\left(\frac{2}{c\sigma}(z'-R)+\frac{\tau}{c\sigma}\right)-\mathrm{erf}\left(\frac{2}{c\sigma}(z'-R)-\frac{\tau}{c\sigma}\right)\right] \quad (18)$$

is the function describing spatial resolution, $\mathrm{erf}(x)=(2/\sqrt{\pi})\int\limits_0^x d\xi\,e^{-\xi^2}$ is the probability integral. The function $Q_S(z')$ is the maximum at $z'=R$ and $\int\limits_{-\infty}^{\infty}dz'\,Q_S(z')=1$. Having defined the longitudinal size of the sounding volume Δz by the expression for

$$\Delta z=\int\limits_{-\infty}^{\infty}dz'\,Q_S(z')/Q_S(R)=Q_S^{-1}(R),$$

we have from Eq. (18) that

$$\Delta z=\frac{c\tau}{2}/\mathrm{erf}(\tau/2\sigma). \quad (19)$$

Calculations by Eq. (19) show that at $\sigma=120$ ns and $T_S=20$ ns, $M=16$ ($\tau=320$ ns) the value $\Delta z=51$ m. Approximately the same result follows from the estimate of longitudinal size of the volume sounded by the $Q_S(z')/Q_S(R)$ decrease to half maximum. It should be noted that for the same values of the parameters σ and τ the estimate of Δz by equation $\Delta z=(\ln 2)^{1/2}c\sigma+c\tau/2$ (Ref. 5) gives the value 79 m,

that is about one and a half times greater than Δz estimate by Eq. (19).

3.2. Maximum likelihood method

Estimation of $V_D(R)$ velocity by maximum likelihood supposes the construction of a logarithmic likelihood function $L(V)$ from the measured values $Z_m = Z(mT_S)$ and determination of the value $V = V_D(R)$, at which $L(V)$ takes its maximum. Neglecting the random character of wind velocity, the recorded signal Z_m can be considered as a nonstationary (due to wind inhomogeneity: $V_r(z') \neq \text{const}$) Gaussian process. For a Gaussian process the function $L(V)$ can be presented as[19,20,17]

$$L(V) = -2\mathrm{Re}\left[\sum_{m=0}^{M-1}\left(\sum_{l=0}^{M-m-1} Z_l Z^*_{l+m}\Lambda_{l,l+m}\right)\exp\left(-j\frac{4\pi}{\lambda}VT_S m\right)\right] +$$

$$+ \sum_{m=0}^{M-1} |Z_m|^2 \Lambda_{m,m} + \ln(\det\Lambda) - M\ln\pi, \qquad (20)$$

where $\Lambda = \{\Lambda_{m,l}\} = \mathbf{B}_z^{-1}$ is the inverse correlation matrix, $\mathbf{B}_z = \{|B_z(mT_S, lT_S)|\}$. In this paper for $B_z(mT_S, lT_S)$ we used Eq. (8). The estimate of $V_D(R)$ obtained in such a way can, by analogy with Eq. (14), be presented as a sum of radial wind velocity $V_a(R)$ averaged over the volume sounded and error in the velocity estimate $V_e(R)$ due to fluctuations of the scattered wave and noise.

A more detailed analytical consideration of the CFA and ML methods proves to be possible only in a limited case $M \to \infty$. Therefore further analysis was done using numerical modeling of lidar signal and its processing.

4. NUMERICAL MODELING OF THE SIGNAL

Signal was modeled by the following scheme.[21,22] The propagation path of a Gaussian sounding pulse was divided into n_L thin layers, and signal mT_S recorded at some time moment was considered as a sum of contributions from all these layers and noise

$$Z(mT_S) = \left(\frac{SNR}{2\sqrt{\pi}}\frac{\Delta p}{p}\right)^{1/2}\sum_{k=0}^{n_L} a(k+ml)\times$$

$$\times\exp\left\{-\frac{1}{2}\left(\frac{\Delta p}{p}\right)^2\left(\frac{n_L}{2}-k\right)^2 -\right.$$

$$\left. - j\frac{4\pi}{\lambda}mT_S V_r(\Delta p(k+ml))\right\} + \frac{1}{\sqrt{2}}n_m, \qquad (21)$$

where Δp is layer depth, $p = \sigma c/2$; $l = [cT_S/(2\Delta p)]$. The number of layers n_L in modeling was taken equal to $n_L = [4\sqrt{2}p/\Delta p]$. To obtain random values of $Z(mT_S)$, Eq. (21) was used for generating independent complex random values $a(k)$ and n_m with real and imaginary parts distributed according to the Gaussian law with the zero mean and unit variance, as well as real random values of wind velocity $V_r(\Delta pk)$. The values $V_r(\Delta pk)$ were obtained from the spectrum of unit complex (Gauss) white noise by multiplying its components by coefficients meeting the spectral density of turbulent fluctuations of wind velocity in the atmosphere

$$S_r(\varkappa) = \int_{-\infty}^{\infty} dr <\tilde{V}_r(R+r)\,\tilde{V}_r(R)> e^{-2\pi j\varkappa r},$$

where $\tilde{V}_r = V_r - <V_r>$, and by applying the inverse Fourier transform. In the results calculated below we used the Karman model[23] for $S_r(\varkappa)$

$$S_r(\varkappa) = 2\sigma_r^2 L_V/[1 + (8.43\,\varkappa L_V)^2]^{5/6}, \qquad (22)$$

where L_V is the integral correlation scale of wind velocity (outer scale of turbulence). At high frequency $\varkappa L_V > 1$, the spectral density $S_r(\varkappa)$ obeys the Kolmogorov–Obukhov law[24]

$$S_r(\varkappa) = 0.0375\,C_K\,\varepsilon^{2/3}\,\varkappa^{-5/3}, \qquad (23)$$

where $C_K \approx 2$ is the Kolmogorov constant, ε is the turbulence energy dissipation rate. From Eqs. (22) and (23) we have the relation between ε, σ_r^2 and L_V in the form

$$\varepsilon = \frac{1.887}{C_K^{3/2}}\frac{\sigma_r^3}{L_V}. \qquad (24)$$

Signal was modeled for $\lambda = 2$ μm, $\sigma = 120$ ns, $T_S = 20$ ns, and $\Delta p = 0.3$ m. In this case $p = 18$ m, $n_S = 340$, and $l = 10$.

5. ESTIMATION OF THE TURBULENT ENERGY DISSIPATION RATE

In order to analyze the possibilities of lidar sounding of dissipation rate ε, let us consider the structure function of the Doppler estimate of the velocity:

$$D(r) = E\{[\tilde{V}_D(R+r) - \tilde{V}_D(R)]^2\},$$

where $\tilde{V}_D = V_D - <V_D>$; $E\{A\} = <\overline{A}>$.

Taking into account that $V_a(R)$ and $V_e(R)$ are independent,[5,22] the structure function $D(r)$ can be presented as

$$D(r) = D_a(r) + D_e(r), \qquad (25)$$

where $D_a(r) = <[\tilde{V}_a(R+r) - \tilde{V}_a(R)]^2>$ is the spatial structure function of the radial wind velocity averaged

over the volume sounded, $D_e(r) = E\{[\tilde{V}_e(R+r) - \tilde{V}_e(R)]^2\}$ is the structure function of the error in the Doppler velocity estimate. In the case of a Gaussian sounding pulse, we have for $D_a(r)$, from Eq. (15), that

$$D_a(r) = 2\int_{-\infty}^{\infty} d\varkappa\, S_r(\varkappa)\, H(\varkappa)\, [1 - \cos(2\pi\varkappa r)], \qquad (26)$$

where

$$H(\varkappa) = \exp\left\{-\frac{1}{2}(\pi c\sigma\varkappa)^2\right\}\left[\frac{\sin(\pi c\tau\varkappa/2)}{\pi c\tau\varkappa/2}\right]^2 \qquad (27)$$

is the transfer function of low-frequency spatial filter. In the inertial interval of turbulent inhomogeneities scales $r \ll L_V$, in Eq. (26) we can use Eq. (23) for $S_r(\varkappa)$, so in this case $D_a(r) \sim \varepsilon^{2/3}$.

The structure function $D_e(r)$ can be presented as

$$D_e(r) = 2[\sigma_e^2 - B_e(r)], \qquad (28)$$

where $B_e(r) = E\{\tilde{V}_e(R+r)\,\tilde{V}_e(R)\}$ and $\sigma_e^2 = B_e(0)$ are respectively the correlation function and the variance of error in the Doppler velocity estimate. Numerical analysis shows that integral scale of the correlation of this error at $L_e \sim \Delta z$, and at $r \gg \Delta z$ the function $D_e(r) = 2\sigma_e^2$.

Thus, it follows from Eqs.(25)–(28) and (23) that at

$$\Delta z \ll r \ll L_V \qquad (29)$$

$D(r)$ is described by the asymptotic formula

$$D(r) = C_K\, \varepsilon^{2/3}\, r^{2/3} - D_0 + 2\sigma_e^2, \qquad (30)$$

where

$$D_0 = 0.15\, C_K\, \varepsilon^{2/3} \int_0^{\infty} d\varkappa\varkappa^{-5/3}[1 - H(\varkappa)]. \qquad (31)$$

Then, for estimating the dissipation rate $\hat{\varepsilon}$ we obtain

$$\hat{\varepsilon} = \left[\frac{\hat{D}(r_2) - \hat{D}(r_1)}{(r_2^{2/3} - r_1^{2/3})\, C_K}\right]^{3/2}, \quad \Delta z \le r_{1,2} \ll L_V, \qquad (32)$$

where $\hat{D}(r_i)$ is the estimate of the velocity structure function, $i = 1, 2$. If the condition

$$C_K\varepsilon^{2/3}(r_2^{2/3} - r_1^{2/3}) \gg [E\{[\tilde{D}(r_2) - \tilde{D}(r_1)]^2\}]^{1/2}$$

is true, then for the variance of relative error in turbulence energy dissipation rate estimate $\sigma_\varepsilon^2 = E\{[(\hat{\varepsilon} - \varepsilon)/\varepsilon]^2\}$ we can find the asymptotic expression from Eq. (32):

$$\sigma_\varepsilon^2 = \frac{9}{4}\,[C_K\,\varepsilon^{2/3}(r_2^{2/3} - r_1^{2/3})]^{-2} E\{[\tilde{D}(r_2) - \tilde{D}(r_1)]^2\}, \qquad (33)$$

where $\tilde{D}(r_i) = \hat{D}(r_i) - D(r_i)$, $i = 1, 2$.

Assuming that the structure function $\hat{D}(r_i)$ is the result of averaging of n_a square differences of Doppler velocity estimates obtained during the measurement time in the given sounding section along z' axis and considering the condition (29) is true (sounding altitude ε is high), for the relative error σ_ε we obtain

$$\sigma_\varepsilon = \frac{6}{C_K\,\varepsilon^{2/3}\,(r_2^{2/3} - r_1^{2/3})}\,\frac{\sigma_e}{\sqrt{n_a}} \times$$

$$\times\left[\sigma_e^2 + \frac{C_K}{2}\,\varepsilon^{2/3}\,(r_2^{2/3} + r_1^{2/3} - \frac{9}{10}\,(\Delta z)^{2/3})\right]^{1/2}. \qquad (34)$$

Then it follows that at $\varepsilon = 10^{-3}$ m^2/s^3, $\Delta z = 50$ m, $r_1 = 100$ m, $r_2 = 400$ m and $\sigma_e = 1$ m/s, to obtain the estimate $\hat{\varepsilon}$ with 20% error, one needs to use $n_a \approx 3500$ points for averaging when estimating $\hat{D}(r_i)$.

When measurements are performed in the ground atmospheric layer or at low altitudes of the boundary atmospheric layer, the outer scale of turbulence L_V may be comparable with the longitudinal size of the volume Δz sounded, and the condition (29) will not hold true. In this case the parameter ε should be estimated from the results of measuring the function[22]

$$D_P(r) = E\{[\tilde{V}_D^{(1)}(R+r) - \tilde{V}_D^{(2)}(R)]^2\}, \qquad (35)$$

where superscripts (1) and (2) denote the velocity estimates from responses to two subsequent sounding pulses. In this case the pulse repetition frequency must be sufficiently high for the condition of frozen turbulence, to hold $V_a^{(1)}(R) \approx V_a^{(2)}(R)$. Then we can take $V_D^{(i)} \approx V_a(R) + V_e^{(i)}(R)$ where $i = 1, 2$. Taking into account that $V_a(R)$, $V_e^{(1)}(R)$ and $V_e^{(2)}$ are independent, from Eq.(35) we have

$$D_P(r) = 2\sigma_e^2 + D_a(r). \qquad (36)$$

As follows from Eq. (36) that $D_P(0) = 2\sigma_e^2$.

Let us introduce $\Delta r = cT_S/2$ for the distance between two velocity estimates (for $T_S = 20$ ns, $\Delta r = 3$ m). The estimate $\hat{\varepsilon}$ can be obtained from solution of the set of equations (the least squares method):

$$\begin{cases} \dfrac{\partial\rho_0(\alpha, \beta)}{\partial\alpha} = 0, \\ \dfrac{\partial\rho_0(\alpha, \beta)}{\partial\beta} = 0, \end{cases} \qquad (37)$$

where

$$\rho_0(\alpha, \beta) = \sum_{m=0}^{M'} [\hat{D}_P(m\Delta r) - \alpha^2 - \beta^2 F_a(m\Delta r)]^2; \qquad (38)$$

$M'\Delta r \ll L_V$, $\hat{D}_P(m\Delta r)$ is the estimate of function (35), $\alpha = \sqrt{2}\,\hat{\sigma}_e$; $\beta = (\hat{\sigma})^{1/3}$; $F_a(m\Delta r) = D_a(m\Delta r)/\varepsilon^{2/3}$ is the function described by Eqs. (26), (27), and (23). In this case one should take only real (at $\alpha^2 > 0$ and $\beta^2 > 0$ non zero) solutions of the set (37).

6. RESULTS OF NUMERICAL MODELING AND DATA PROCESSING

Numerical modeling of signal was done for a 2-μm-wavelength pulsed Doppler lidar with $\sigma = 120$ ns and $T_S = 20$ ns at different values of signal-to-noise ratio, *SNR*. Separate random values of radial wind velocity with zero mean ($\langle V_r \rangle = 0$) were modeled at an interval $L_R = 2048 \cdot \Delta p = 614.4$ m at $\Delta p = 0.3$ m. The velocity V_r was modeled for the case of Karman spectrum (22) with $\sigma_r = 1$ m/s and $L_V = 150$ m. In this case, according to Eq. (24), the turbulence energy dissipation rate $\varepsilon = 4.45 \cdot 10^{-3}\text{m}^2/\text{s}^3$.

For a separate pulse, under the assumption that the pulse is within the range ΔL_R on the interval $[0, L_R]$, 64 values of the complex signal $Z(mT_S)$ were modeled, from which at $M = 16$ ($\tau = 320$ ns, $c\tau/2 = 48$ m) 49 values of velocity V_D were estimated by CFA and ML methods. Under the assumption that the pulse repetition rate is 10 Hz, we supposed that at every subsequent pulse the range ΔL_R shifts at a distance 0.9 m with respect to distribution of random wind pattern along the sounding path. For the outer scale of turbulence $L_V = 150$ m, this corresponds, under the assumption of frozen turbulence, to about 15 s time of radial velocity correlation. One pattern of wind V_r with a selected length was used for 350 shots. Presented below are the results, for every 1000 V_r. patterns were modeled. Total number of V_D estimates obtained using each estimation method (CFA and ML) was: $1000 \times 350 \times 49 = 1.715 \cdot 10^7$. In the case of low *SNR*, to obtain the stable statistical characteristics, even a greater number of sample data was used.

Figure 1 shows the results of calculation of the functions $D(r)$, $D_P(r)$ and $D_a(r)$ by modeling at $SNR = 100$ (symbols) and calculation of $D(r)$ and $D_a(r)$ by Eq. (26) (solid and dashed curves). Here, the closed triangles, squares and circles are for the data processed with CFA method, while the open triangles, squares and circles are for the data processed using ML method. Triangles are for $D_P(r)$, stars and circles are for $D(r)$, and squares are for $D_a(r)$. Curves *1* and *2* correspond to calculations of the structure function of the velocity measured at a point for Karman spectrum (22) (solid curve) and for Kolmogorov spectrum (23) (dashed curve). Curves *3* and *4* show the $D_a(r)$ calculation by Eq. (26) taking into account averaging over the volume sounded. Comparing the curves *1* and *2* (or *3* and *4*) one can see that for the data presented the length of turbulence inertial range r_{in}, where this curves must be closed, is limited by about 50 m, i.e. it is comparable with longitudinal size of the volume sounded $r_{\text{in}} \approx \Delta z$. Therefore, to estimate the turbulence energy dissipation rate, we used the algorithm (37), (38). Discrepancy between the curves *1* and *3* illustrates the influence of spatial averaging of radial wind velocity over the volume sounded.

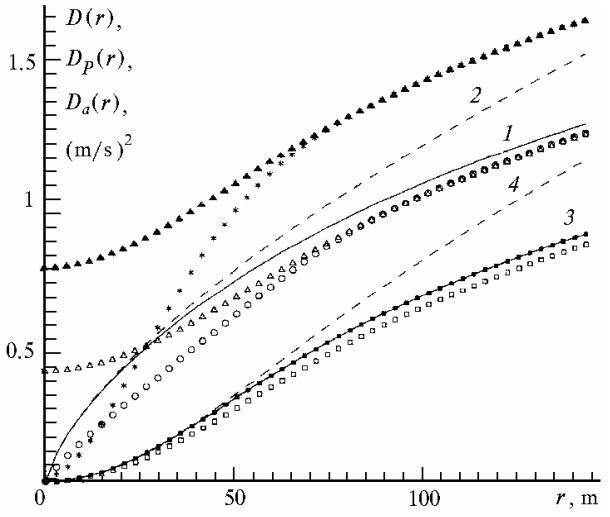

FIG. 1. Functions $D(r)$, $D_P(r)$, and $D_a(r)$. Curves 1 and 2 are for calculation of the structure function $D(r)$ for velocity measured at a point for the case of Karman (1) and Kolmogorov (2) spectra; curves 3 and 4 are for calculation of structure function $D_a(r)$ by Eq. (26) for the same spectrum models, respectively; ▲, Δ – $D_P(r)$; ■, □ – $D_a(r)$; ∗, ○ – $D_a(r)$; ▲, ■, ∗ – CFA method; Δ, □, ○ – ML method.

One can see from Fig. 1 that the variance of the error in the velocity estimate $\sigma_e^2 = D_P(0)/2$ for the case of CFA method is greater than for ML method. It is in agreement with the known results.[17] With increasing r the difference between $D_P(r)$ and $D(r)$ vanishes that is due to decreasing level of correlation between the errors $V_e(R + r)$ and $V_e(R)$. Figure 2 shows the results calculated for correlation coefficient of velocity estimate errors $K_e(r) = [D_P(r) - D(r)]/D_P(0)$ by Eqs. (25), (28), and (36) at different *SNR*. One can see that the effective scale of the correlation between the errors $\sim \Delta z = 51$ m, and it decreases with decreasing *SNR*.

According to the data from Fig. 1, the calculations of $D_a(r)$ by Eqs. (26), (27), (22) and on the basis of modeling with the use of CFA method for wind velocity estimation give, as was shown earlier,[22] the same result within a wide range of *SNR* values (up to $SNR = 1$). At the same time, the structure function $D_a(r)$, calculated with ML method has, in comparison with the results of calculation, underestimated values. As a result, the dissipation rate estimate $\hat{\varepsilon}$, obtained by solving the system of equations (37) with the use of Eqs. (26), (27) and (23) for $F_a(m\Delta r)$, should have been biased (regular underestimation). Figure 3 shows the structure functions $D_a(r)$ obtained with the use of CFA and ML methods at different values of signal-to-

noise ratio. Dashed curve is here for the asymptotic $D_a(m\Delta r) = \varepsilon^{2/3} F_a(m\Delta r)$, where $F_a(m\Delta r)$ is used in Eq. (38) when estimating $\hat{\varepsilon}$. It is seen from Fig. 3 that with a decrease in *SNR* the difference between $D_a(r)$ obtained in different ways decreases and, consequently, the bias of error $\hat{\varepsilon}$ in the case of ML method must become smaller.

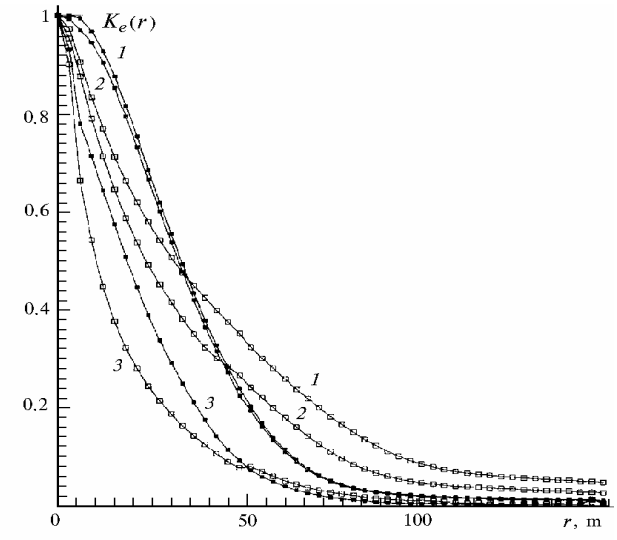

FIG. 2. Correlation coefficient for the error of wind velocity estimate. ■ – CFA method; □ – ML method; SNR = 1000 (1), 100 (2), and 10 (3).

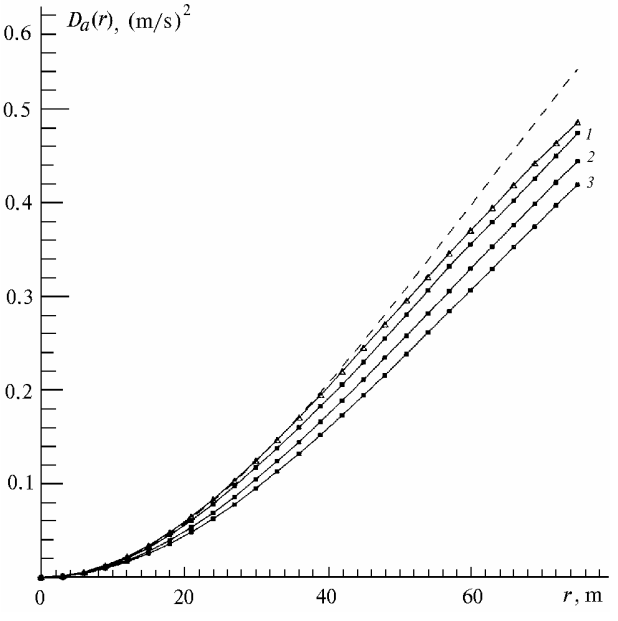

FIG. 3. Structure function $D_a(r)$. Dashed curve is for calculation by Eq. (26) for Kolmogorov spectrum; ▲ – CFA method; ■ – ML method; SNR = 10 (1), 100 (2), and 1000 (3).

The modeling results at small values of *SNR* demonstrate the impossibility to obtain $\hat{\varepsilon}$ estimate with an acceptable accuracy from the function $\hat{D}_P(r)$ measured in real time without the use of special procedures of data processing. Figure 4 shows, as an example, the distribution functions of the probability density $P_V(V_D)$ of velocity estimates by ML method (curve *1*) and CFA method (curve *2*) at $SNR = 1$. It is seen that CFA method gives a more diffuse distribution as compared to ML method. For the case of CFA method at homogeneous wind $V_r = \text{const}$ Ref. 25 presents the asymptotic equation for $P_V(V_D)$. When using the ML method, the function $P_V(V_D)$ is well approximated by Gaussian distribution (it is shown in Fig. 4 as dashed curve), that describes, according to the terminology used in Ref. 17, the distribution of "good" velocity estimate, on a uniform pedestal, being the distribution of "bad" (or obviously false) velocity estimate.

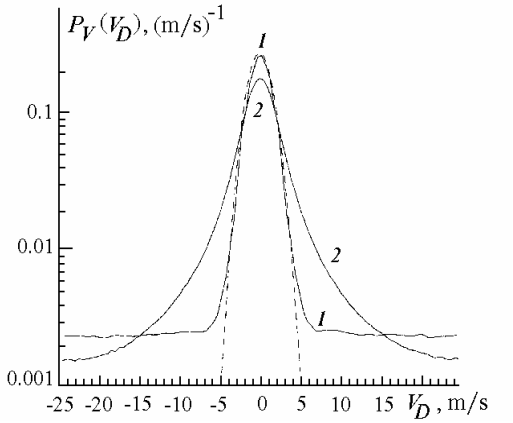

FIG. 4. Probability density function for the velocity estimates by ML method (curve 1) and CFA method (curve 2); dashed curve is for the Gaussian distribution.

The obtained arrays of V_D estimates allow us to find the probability density $P_V(V_D)$ and to separate the range of velocities V_D with center at the maximum value of $P_V(V_D)$. In our case, optimal is the velocity range from −5 m/s to +5 m/s. Then, in order to cut off the "bad" velocity estimates, the estimates V_D, not falling within this range, were discarded. Taking into account that V_D values are used for calculation of the spatial function $D_P(m\Delta r)$, Eq. (35), data corresponding to a pair of neighbor shots, where at least one value is out of the above range, are all discarded. Such procedure of data filtration has certainly a disadvantage that data become less in number, especially when using CFA method. Nevertheless it leads to a more accurate estimate of $\hat{\varepsilon}$ than that when using all (including "bad") estimates V_D, including the case of applying "incoherent" averaging. We used the described procedure at $SNR \le 10$.

From the obtained large data array of V_D values, we estimated the function $\hat{D}_P(m\Delta r)$ by varying the number of shots from 350 to 17500. For the pulse repetition rate of 10 Hz it corresponded to averaging time T from 35 s to 1750 s ≈ 30 minutes. Then, with the use of thus obtained $\hat{\varepsilon}$ values, we calculated the dependence of

relative error in the dissipation rate estimate σ_ε on the time of averaging T. The relative error in calculation of σ_ε itself was below 10%. Figure 5 shows the dependences of σ_ε (in per cent) on the averaging time T for estimating the velocity V_D by ML method (*a*) and CFA method (*b*). As seen, the error σ_ε decreases monotonically with increasing T in the considered range of averaging time, with the exception for the cases described by curves *1* and *2* in Fig. 5*a*. Here the saturation to certain levels takes place because of the bias resulting from $\hat{\varepsilon}$ estimation with ML method in the case of large *SNR* (due to incorrect set of the function $F_a(m\Delta r)$ to fit the Eq. (38)). The large error σ_ε observed in the case of CFA method at $SNR = 1$ (Fig. 5*b*, curve *5*) is due to a significant "loss" of data after applying the filtration procedure described above.

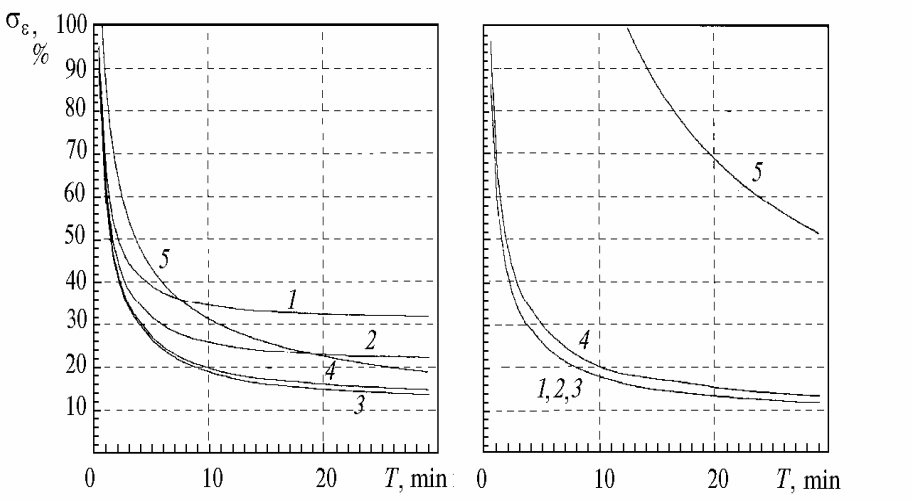

FIG. 5. Relative error in estimate of the turbulence energy dissipation rate as a function of averaging time using ML method (a) and CFA method (b) for SNR = 1000 (1), 100 (2), 10 (3), 5 (4), 1 (5).

Figure 6 shows the error σ_ε as a function of signal-to-noise ratio with the averaging time $T = 30$ min.

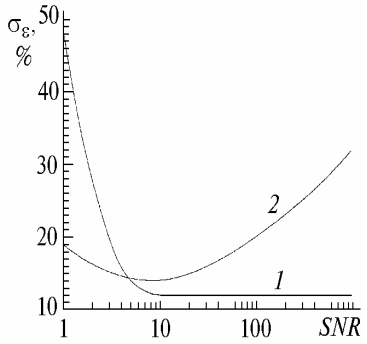

FIG. 6. σ_ε vs SNR for 30-minute averaging time; ML method (1), CFA method (2).

As follows from the figure, to estimate the turbulence energy dissipation rate in the case of high $SNR \geq 5$, CFA method gives better results, while at $SNR < 5$ the best result is achieved by ML method.

7. CONCLUSION

Thus, in this paper for the case of a small, in comparison with the outer scale of turbulence, longitudinal size of a lidar volume the asymptotic formula (34) was derived, that allows one to estimate the size of statistical sample needed to reach given accuracy of estimate of turbulence kinetic energy dissipation rate from pulsed lidar data. It is shown that the method of wind velocity estimation by argument of correlation function gives smaller error at large values of signal-to-noise ratio, while the method of maximum likelihood works better at low *SNR*. It follows from the results of numerical modeling that, at a sufficiently great number of sample data, the relative error in estimate of turbulence energy dissipation rate with a pulsed Doppler lidar must be no greater than 15–20% at $SNR \geq 1$.

REFERENCES

1. F.F. Hall, R.M. Huffaker, R.M. Hardesty, et al., Appl. Optics **23**, No.15, 2503–2506 (1984).
2. S.W. Henderson, C.P. Hale, J.R. Magee, et al., Optics Lett. **16**, No. 10, 773–775 (1991).
3. T. Cal-Chen, Mei Xu, and W.L. Eberhard, J. Geophys. Res. **97**, No. D17, 18409–18423 (1992).
4. J.G. Hawley, R. Targ, S.W. Henderson, et al., Appl. Optics **32**, No. 24, 4557–4568 (1993).
5. R. Frehlich, S.M. Hannon, and S.W. Henderson, J. Atmos. Oceanic Technol. **11**, No. 6, 1517–1528 (1994).
6. S.M. Hannon, J.A. Thomson, S.W. Henderson, and R.M. Huffaker, Air Trafic Control Technologies. Proc. SPIE **2464**, 94–102 (1995).
7. R. Frehlich, S.M. Hannon, and S.W. Henderson, Appl. Optics **36**, No. 15, 3491–3499 (1997).

8. V. Klein, J. Roths, and ”. Hilber, in: *Proceedings of 9th Conference on Coherent Laser Radar*, (1997), pp. 281–284.
9. V.A. Banakh, Ch. Verner, N.N. Kerkis, F. Kopp, and I.N. Smalikho, Atmos. Oceanic Optics **8**, No. 12, 955–959 (1995).
10. I.N. Smalikho, Atmos. Oceanic Optics **8**, No. 10, 788–793 (1995).
11. V.A. Banakh, Ch. Werner, F. Kopp, and I.N. Smalikho, Atmos. Oceanic Optics **9**, No. 10, 849–853 (1996).
12. V.A. Banakh, Ch. Werner, F. Kopp, and I.N. Smalikho, Atmos. Oceanic Optics **10**, No. 3, 202–208 (1997).
13. V.A. Banakh and I.N. Smalikho, Atmos. Oceanic Optics **10**, Nos. 4–5, 295–302 (1997).
14. R. Frehlich and M.J. Kavaya , Appl. Optics **30**, No. 36, 5325–5352 (1991).
15. R. Frehlich, Appl. Optics **33**, No. 27, 6472–6481 (1994).
16. A. Van der Zil, *Noise in Measurements* [Russian translation] (Mir, Moscow, 1979), 230 pp.
17. R. Frehlich and M.J. Yadlowsky, J. Atmos. Oceanic Technol. **11**, 1217–1230 (1994).
18. R.J. Doviak and D.S. Zrnic, *Doppler Radar and Weather Observations* (Academic Press, 1993), 562 pp.
19. H.L. Van Trees, *Estimation and Modulation Theory. 1. Detection, Estimation, and Linear Modulation Theory* (Wiley, New York, 1968).
20. D.S. Zrnic, IEEE Trans. Geosc. Electr. **GE-17**, No. 4, 113–128 (1979).
21. P. Salamitou, A. Dabas, and P. Flamant, Appl. Optics **34**, No. 3, 499–506 (1995).
22. R. Frehlich, J. Atmos. Oceanic Technol. **14**, 54–75 (1997).
23. N.K. Vinnichenko, N.Z. Pinus, S.M. Shmeter, and G.N. Shur, *Turbulence in the Free Atmosphere* (Gidrometeoizdat, Leningrad, 1976), 287 pp.
24. A.S. Monin and A.M. Yaglom, *Statistical Hydromechanics*, Part 2 (Nauka, Moscow, 1967), 720 pp.
25. D.S. Zrnic , IEEE Trans. Aerosp. and Electron. Syst. **AES-13**, No. 4, 344–354 (1977).